Fluid Structure Interaction With Beam Models

Diogo José Martins Cerdeira
diogo.cerdeira@tecnico.ulisboa.pt

Instituto Superior Técnico, Lisboa, Portugal

July 2022

Abstract

In the past several years, the demand for wind energy has increased with the rising need for sustainable energy generation, which led to the escalation of power and size of the wind turbines. Aiming to study these new prototypes at realistic full-scale with efficiency, an interface is developed between a beam structural representation of the body and the fluid mesh, expanding the compatibility of an already existent Fluid-Structure Interaction (FSI) module to beam elements. Aiming to remove the dependency on other software, a solver responsible for generating the input data regarding the beam models is created, based on the finite element method. This new structural solver is then successfully validated in a FSI context with a 2D benchmark, as well as the implemented interface coupling. Obtained deviations of the results were attributed to the lack of refinement of the outer mesh that interacts with the fluid. Limitations in this coupling were also identified, as it was founded that a lack of refinement from the beam grid in comparison with the outer mesh creates irregular surfaces in the body, possibly leading to divergence. Planning to simulate the DTU 10MW rotor, rigid simulations are executed with Sliding Grids and Absolute Formulation Method approaches, with the former presenting more reliable results. The structural input data of the FSI module for a blade of the rotor is also formulated successfully with the developed beam solver and the combination of these advancements should lead to successful future simulations of the turbine, with a parallelized code.
Keywords: Aeroelasticity, Fluid Structure Interaction, Interface coupling, CFD

1. Introduction

Nowadays, there is a remarkable development of the wind power technology in Europe, in alignment with the rising need for sustainability in electrical power generation. In order to cope with a consequent upscaling of the wind turbines, aeroelastic effects start to play a major role in the simulations that cater to the design and evaluation of those machines.

While traditional Computational Fluid Dynamics (CFD) approaches tend to address the wind turbines as rigid models, blade deflections do have an appreciable impact on the turbine performance and should be taken into account in the design and evaluation of FOWTs.

This added structural nature to the problems at hand leads to Fluid Structure Interactions (FSI) simulations, where structural models have to be able to capture the complex features of FOWTs, while still achieving reasonable computational costs. An approach that addresses the efficiency of these studies is the use of beam and shell elements to represent the blades of the rotor. In the scope of this work, one will focus on the former type of element.

In an FSI context, non-linear Timoshenko beam elements have been used, for instance, by Yu and Kwon [1] with the intent of simulating a Rotor-Nacelle Assembly (RNA) and the full machine of the DTU 10MW. Hence, with similar goals in mind, a framework is outlined: develop a module capable of generating the structural data for a beam model representing the body at study and establish a coupling interface between that structural grid and the fluid mesh on an already existent FSI module of ReFRESCO, a Reynolds-Averaged-Navier–Stokes (RANS) solver.

This CFD code has already been successfully tested with Solid elements by Bronswijk [2], applied to flexible marine propeller simulations. The current work presents an opportunity not only to expand on its compatibility with other elements but also to remove its reliance on external software to obtain the structural data of the model.

Having implemented these advancements, the developed work is then validated with a two-dimensional (2D) benchmark, leading up to the main objective of the study, a full scale simulation of the DTU 10MW RWT rotor with a flexible blade.

2. Fluid Dynamics Model

Aiming to compute the aerodynamic loads to which the body is submitted in an accurate CFD environment, the RANS solver ReFRESCO, developed at MARIN, is used in this work.

2.1. RANS solver

ReFRESCO solves multiphase incompressible viscous flows through the Navier-Stokes (NS) equations, recurring to a numerical approach where a discretization of the domain with the finite volume method is conducted, using cell centred collocated variables. The coupled non-linear equations are solved using the Picard linearization and a SIMPLE algorithm [3].

Time iterations are performed implicitly through first or second-order backward schemes, with a typical solving process in ReFRESCO containing three iteration loops, denoted as the time loop, the outer loop and the inner loop. At each time loop, the outer-loops account for non-linearity and deferred corrections, containing within them the inner loops, where the momentum, pressure correction, velocity and turbulence model equations are solved using the parallelized-solvers library PETSc [3]. The process comes to an end and exits the loops when the suitable convergence criteria or the maximum number of outer loops are met.

Additionally, these equations are complemented by turbulence models that account for turbulence fluctuations of the flow, with a variety of RANS options. The $k - \sqrt{k}L$ turbulence model is the employed for the simulations of the rotor of the turbine, as it yields more stable simulations, without necessarily losing accuracy. It is composed by two main equations: a transport equation for the turbulent kinetic energy k and one for $\sqrt{k}L$, where L constitutes an integral length scale.

2.2. Grid methods

The CFD solver also features deforming, moving and sliding grids. The deforming grids are inherently associated to FSI simulations and are used in any test case of this work that involves flexible bodies. The moving and sliding grids are adopted particularly in the DTU 10MW RWT model, with the intent of simulating the rotation of the its rotor. Two distinct approaches are taken in this work to depict that rotation movement: the Absolute Formulation Method (AFM) and Sliding Grids (SG).

In the first formulation, RANS equations are solved in the moving reference frame but using variables written in terms of absolute or inertial reference frame quantities [3]. This formulation implies that the rotor geometry remains static, which facilitates the FSI process and its interface coupling, even if at a cost of a weaker depiction of the unsteadiness of the flow.

In regards to the SG, this methodology allows that, instead of rotating the entire computational domain, only an inner cylindrical sub-domain that envelops the rotor's geometry undergoes the rotation motion, inside another cylindrical sub-domain. This exterior sub-domain contains a cutout with the dimensions of the inner one, so they can fit into one another, sharing a common interface. Therefore, these two grids do not overlap each other and are in relative motion, with an imposed continuity of kinematics at the shared interface.

3. Fluid Structure Interaction

The FSI problematic encompasses the coupling between the structural model of a body and the surrounding fluid, in order to solve the equations of motion of the body at study. An FSI module was implemented in ReFRESCO by Jongsma and Windt [4] and this Section pertains to expand its compatibility features to structural models constituted by beam elements.

3.1. FSI algorithm

The aforementioned FSI module takes a partitioned strong coupling approach, where the fluid and structural problems are solved separately and the coupling iterations are performed each time step until convergence is met.

The process starts with the computation of the loads acting on an interface between non-identical structural and fluid grids, based on external forces and the forces exerted by the flow through pressure and shear stress.

Subsequently, solving the equations of motion of these loads, displacements are obtained in the structural model and can then be used to update the vertices of the CFD mesh through, once again, the Fluid-Structure Interface coupling. Following this process, a grid deform method is applied on the field grid of the flow domain with an identical interpolation to one used on the interface.

At last, an update for the flow solution is computed and the whole procedure is repeated until the convergence criteria defined for the flow method solution on the controls file has been met [4]. In that case, the process can advance to next time step, as shown in the flowchart from Figure 1.

3.2. Interface coupling

Regarding the interface between the two domains, the coupling of fluid and structure equations is usually defined by kinematic and dynamic boundary conditions, given in equations 1a and 1b [5].

$$\boldsymbol{u_f} = \boldsymbol{u_s} \text{ on } \Gamma \tag{1a}$$

$$T_s \boldsymbol{n_s} = T_f \boldsymbol{n_f} \text{ on } \Gamma, \tag{1b}$$

with $\boldsymbol{u}$ representing the displacements, T the stress tensor and $\boldsymbol{n}$ the outward normal of the continuous

interface Γ between the structural (s) and fluid (f) grids. The first condition conveys equal displacements on both domains at Γ, while the second expresses that, on that same interface, the pressure on the fluid mesh is in equilibrium with the structural one.

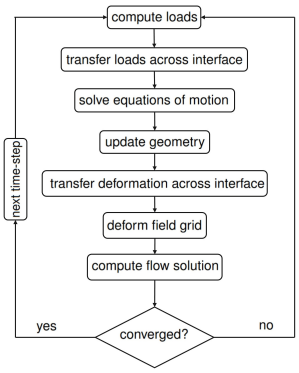

Figure 1: Flow chart representing one time step of an FSI simulation [4].

In order to achieve accurate results, another condition should also be considered: the conservation of global energy over the interface. This conservative coupling approach can be written as seen on Equation 2.

$$\int_{\Gamma_f} \boldsymbol{u_f} \cdot T_f \boldsymbol{n_f}\, ds = \int_{\Gamma_s} \boldsymbol{u_s} \cdot T_s \boldsymbol{n_s}\, ds, \qquad (2)$$

In ReFRESCO, the main method concerning the coupling between the fluid and structural domains corresponds to the Radial Basis Function (RBF) Interpolation, a conservative approach.

3.3. Radial Basis Function Interpolation

The Radial Basis Function Interpolation transfers the quantity of a mesh A to another grid B recurring to a global interpolation function, which results from the sum of basis functions [5], as shown in Equation 3.

$$f_i(x) = \sum_{j=1}^{N_c} \alpha_j \psi(\|x - x_{Aj}\|) + p(x), i = A, B, \quad (3)$$

where to every known data point of mesh A (x_A) corresponds a distinct radial basis function in the form of $\psi(\|x - x_{jc}\|)$ and $f_i(x)$ is the interpolation function that results from their linear combination, for a set of N_c points. Additionally, $p(x)$ is a polynomial whose minimal degree is dependent on the chosen RBF function ψ.

The coefficients α_j are then determined by evaluating the condition on Equation 4 for all data points and by ensuring that the resulting system of linear equations presents positive definiteness.

$$f_A(x_{Aj}) = F_{Aj}, j = 1, ..., N_c, \qquad (4)$$

with F_{Aj} as the discrete values of f_A at the interface of mesh A.

Through those conditions, eventually it is possible to write the system in equation 5, from which is possible to extract the values on mesh B (F_B).

$$F_B = \begin{bmatrix} \Phi_{BA} & Q_B \end{bmatrix} \begin{bmatrix} \alpha \\ \beta \end{bmatrix}, \qquad (5)$$

where Φ_{BA} is a square matrix containing the evaluation of the basis function $\psi(\|x_{Ai} - x_{Bj}\|)$. α contains the coefficients α_j and β the coefficients of the polynomial p, while Q_B is a matrix where each row j has the form $\begin{bmatrix} 1 & x_{Aj,Bj} & y_{Aj,Bj} & z_{Aj,Bj} \end{bmatrix}$ [5].

After obtaining the properties of the receiver mesh, in what concerns the update of the interface position, the RBF method is also assisted by the Aitken under-relaxation and a greedy method, in order to ensure stability of the coupled system and tackle computation challenges that arise from the interpolation.

3.4. FSI implementation with beam models

When simulating the behavior of a body through a beam model, the mesh of those elements corresponds to a line along which its nodes are distributed, with a defined cross-section that emulates the body's geometry. However, in order to establish the interaction between the structural and fluid grids with the RBF interpolation method, ReFRESCO uses the interface nodes on the outer surfaces of the structural mesh to transfer the displacements and loads, which poses a challenge when considering a structural grid that is situated internally to the actual body.

With the intent of maintaining the use of the RBF interpolation in the interface coupling of this new problematic, it is necessary to fill in the missing nodes that establish the contact with the fluid and build a new auxiliary structural grid representing the outer surfaces of the body, as seen in Figure 2. The construction of this outer structural mesh is the approach taken in this work.

The presence of this new grid requires the same input data as before, with the addition of a new structural file with the extension *.outernodes* (refer to Figure 3, where the input files are listed, considering ANSYS© their source). This file contains the number of nodes of the outer mesh, boundary conditions (BC) and a listing of the coordinates of all those points, while a file *.intnodes*, in this context, consists on a listing of the coordinates of the nodes from the beam model and respective BC. The mass and stiffness matrices of the beam are supplied through files in Harwell-Boeing (HB) format. A new tag is also added to the main code of ReFRESCO, in order to signal the use of a beam model and thus initiate a different interface coupling.

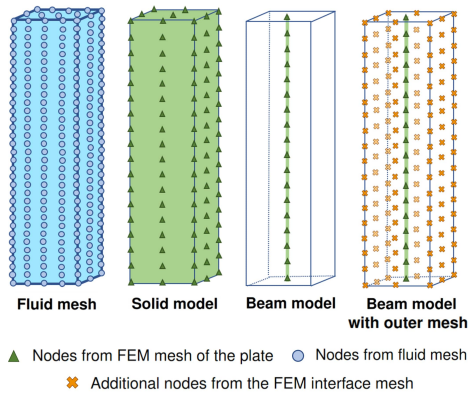

Figure 2: Scheme of fluid and structural grids considered to represent an example body.

3.5. FSI algorithm with beam model

Similarly to the rationale stated in section 3.1, when working with a beam model, the computed fluid mechanics forces are transferred to the structural model so they can be considered when solving the equations of motion of the body. However, in the present case, these forces are interpolated in the outer structural mesh through RBF interpolation and, afterwards, the load applied to each node of that mesh is transferred to the closest node of the beam grid. This transfer is implemented in ReFRESCO through changes of the main code, with modifications on the already existent RBF interpolation function dedicated to loads transfer, as well as on the one responsible for computing the loads contribution of the fluid.

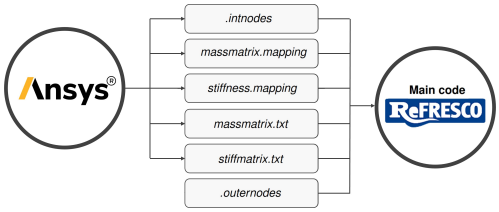

Figure 3: ReFRESCO functioning with structural data from a beam generated by ANSYS© as input.

After the beam nodes receive the loads from the outer mesh, the equations of motion of the beam model can then be solved. Considering that the beam model may include degrees of freedom of rotation in its nodes, another challenge rises: expand ReFRESCO's capabilities to 6 degrees of freedom, allowing the linear system to solve not only displacements, but also rotations. This is achieved through changes in the HB interface function of the main code.

However, these latter results still need to be taken into account on the update of the geometry of the beam because only translations were considered on the original module. In order to tackle this issue, for each update of the geometry, the initial coordinate system is rotated with the computed angles of the previous iteration and the current displacements are applied to the new rotated system. This new update is achieved by applying a rotational matrix $[R_\theta]$ to the entries of translational displacements $\tilde{\boldsymbol{r}}^{\boldsymbol{i}}$, as presented in Equation 6.

$$\boldsymbol{r}^{\boldsymbol{i}} = [R_\theta]\tilde{\boldsymbol{r}}^{\boldsymbol{i}}, \tag{6}$$

This process can be better understood through the flow chart in Figure 4, where the procedure for a single outer iteration is depicted.

After applying the newly computed displacements to the beam geometry, the outer structural mesh also needs to deform, as the discretised flow domain will aim to match the shape of the surface of the object. Therefore, each node of the outer mesh receives the same displacement as the one computed for the closest beam node.

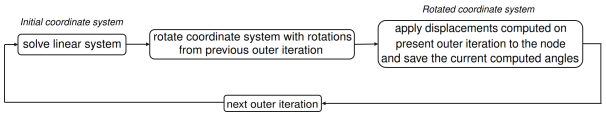

Figure 4: Flow chart of the process for the computed rotations at each outer iteration.

Following this transfer between structural meshes, once again through RBF interpolation, the CFD grid is updated in the interface with the displacements from the new shape of the outer surface of the body. The field grid of the flow is then updated and a new flow solution is finally computed. All this process, depicted in the flow chart of the Figure 5, repeats itself until the imposed convergence criteria is reached.

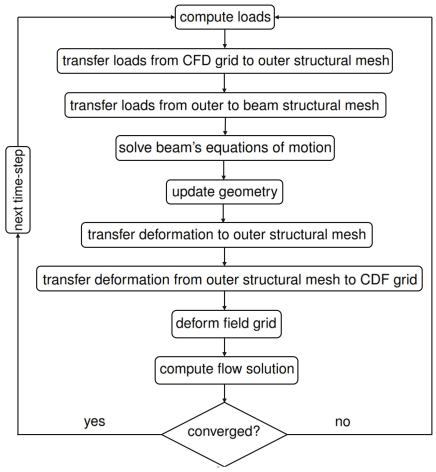

Figure 5: Flow chart representing one time step of an FSI simulation with a beam model.

4. Computational Structural Beam Module (CSBM)

Having developed the interface between the beam models and the CFD grid, the implementation of a module capable of simulating the behavior of a beam constitutes the next objective of this study, which would remove ReFRESCO's dependency on outsourcing the FEM structural process to another software, namely ANSYS©.

4.1. Beam model formulation

When formulating the beam element to be used in the solver, it is essential that the resulting model encompasses relevant structural phenomenons that the blade of a wind turbine suffers, such as axial, bending and torsion deformations.

Having this in mind, a beam element as the one depicted in Figure 6 is adopted for this study.

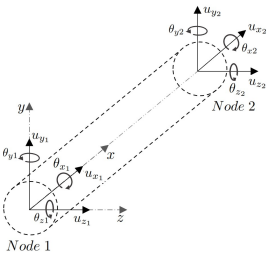

Figure 6: Adopted beam element in local coordinate system.

It can be decoupled in 4 distinct models, based on the work of Reddy [6]:

1. a bar with only axial displacements, whose governing equation is given by:

$$\frac{d}{dx}\left(EA\frac{du_x}{dx}\right) + p(x) = 0, \forall x \in [0, L], \quad (7)$$

where E is the Young's modulus of the material, A is the cross section and u_x is the displacement along the x axis.

2. two Timoshenko beam elements for the xz and xy planes. For the plane xz, the formulation results in the following second order differential equations, for any $x \in [0, L]$:

$$-\frac{d}{dx}\left[GAK_{sh}\left(\theta_y + \frac{du_z}{dx}\right)\right] + q(x) = 0 \quad (8a)$$

$$-\frac{d}{dx}\left(EI_{yy}\frac{d\theta_y}{dx}\right) + GAK_{sh}\left(\theta_y + \frac{du_z}{dx}\right) = 0, \quad (8b)$$

where I_{yy} denotes the area moment about the y axis of the beam, E is the Young's modulus of the material, G the shear modulus, $\theta_y(x)$ is the rotation around the y axis and K_{sh} corresponds to shear correction coefficient. For a bending deformation on the plane xy, I_{yy}, θ_y and u_z turn into I_{zz}, θ_z and u_y, respectively.

3. one torsion element with rotation around the x axis, expressed by:

$$\frac{d}{dx}\left(GJ\frac{d\theta_x}{dx}\right) + m_x = 0, \forall x \in [0, L], \quad (9)$$

with J as the torsional moment of inertia, θ_x the torsion angle around the x axis and m_x the distributed torsion load.

From this superposition of elements, one obtains a three dimensional (3D) beam element with two nodes and six degrees of freedom on each end: three translational and three rotational.

In order to construct the mass and stiffness matrices, the aforementioned equations are combined with shape functions in the potential and kinetic energy equations of the system. Considering the beam formulation already proposed, adequate shape functions and resulting mass and stiffness matrices were extracted from ANSYS© documentation [7], which presents a similar beam element to the one adopted here: the BEAM4.

4.2. Implementation of the beam module

The beam solver is implemented through a user-coding module of ReFRESCO, in Fortran 2005 language, and, working in tandem with the new interface coupling developed for beam elements, it only requires a file *.beam* to provide for the well functioning of the structural portion of the simulation, as presented in Figure 7.

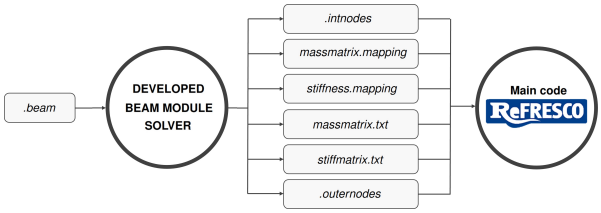

Figure 7: ReFRESCO functioning with structural data provided by the beam solver module as input.

The *.beam* file should contain material data and geometric properties, concerning the cross section of each element of the beam model, as well as information on the coordinates and boundary conditions of the beam mesh and outer structural grid. The material and geometrical properties of elements with non constant cross sections should be averaged with the nodal values. Furthermore, the beam grid is designed with the intent of matching the elastic axis of the body, with its beam nodes passing through the shear centers of predefined cross-sections.

All this information is assimilated by the user code module when the controls of the simulation are being read on ReFRESCO, so that the entire process can take place before the structural files are demanded. After the data is collected, the solver identifies the different elements composing the model and it searches for nodes that belong to more than one element, as repeated nodes on the listing of the mesh represent the same degrees of freedom on the computed matrices. With that goal in mind, a connectivity table is created, keeping track of coincident degrees of freedom from different elements and imposed boundary conditions.

The module then builds the stiffness $[\tilde{K}^i]$ and mass $[\tilde{M}^i]$ matrices for each element with the information previously extracted from the input file and based on the matrices from ANSYS© documentation [7]. Taking into account that those matrices are defined for a local coordinate system, they will need to be transformed to approach a global one, depending on the orientation of the element at study. This is achieved through rotation matrices $[\Gamma^i]$, in the following Equations:

$$[K^i] = [\Gamma^i]^T[\tilde{K}^i][\Gamma^i], \tag{10}$$

$$[M^i] = [\Gamma^i]^T[\tilde{M}^i][\Gamma^i], \tag{11}$$

After applying the transformation of the coordinate system to each elementary matrix, one can finally assemble them into the global matrices of the model. Additionally, the user has the ability to define primary boundary conditions, by stating fixed nodes through the input file *.beam*, and these are considered on the final assembly of the linear systems by nullifying the rows and columns correspondent to the imposed degrees of freedom.

4.3. Validation of the beam solver

For the validation of the beam solver, De Nayer's benchmark [8] is chosen to test the module. The body at study corresponds to an isotropic plate with a quadrangular cross section, fixed on one end, as seen on Figure 8, with some of its relevant properties stated in Table 3.

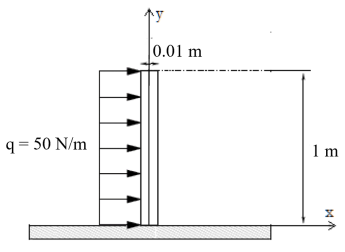

Figure 8: Benchmark for static analysis of the beam model [9].

A linear static analysis is conducted, considering that a distributed load q=50 N/m is applied to the beam, as depicted in Figure 8. A convergence study for a beam model with 200 elements, presented in Table 1, is conducted for this problem, using the BEAM4 element from ANSYS© as a reference.

It is founded that the developed beam module presents itself quite accurate at calculating the deformation when compared with the reference results for this set up. This study is then expanded to the successful testing of the model with other loads and moments, aiming to study its response in regard to different degrees of freedom.

Table 1: Convergence study of the maximum displacement of the beam from De Nayer benchmark.

El. size y[m]	1.0	0.01	0.001
Number of el.	1	100	1000
Aspect ratio	100.0	1.0	0.1
ANSYS©[m]	0.021517	0.021517	0.021517
Beam solver [m]	0.0215	0.0215	0.0215
% Difference	0.000	0.000	0.000

Finally, a modal analysis is executed, with its results presented in Table 2. The obtained natural frequencies by the beam module are very close to the ones from ANSYS©, never surpassing a relative difference of 1%, which verifies the reliability of this solver to represent the behavior of free vibrations for beam elements.

Table 2: Modal analysis of plate with 200 beam elements.

Mode	**CSBM[Hz]**	**ANSYS©[Hz]**	**%Difference**
1^{st}	2.7527	2.7531	-0.0145
2^{nd}	17.232	17.245	-0.0753
3^{rd}	48.172	48.250	-0.162
4^{th}	94.199	94.446	-0.262
5^{th}	155.37	155.90	-0.340

A verification study is also conducted for all the aforementioned results, with extremely low computed uncertainties.

5. Benchmark case

With the intent of validating the new interface coupling and the developed beam model, the already mentioned De Nayer's benchmark [8] is adopted, now in an FSI context, using as reference a solid model that is already validated by Bronswijk [2].

The case in analysis corresponds to a thin flexible quadrangular plate clamped at the bottom wall boundary, located downstream of an incompressible fluid flow with uniform inflow velocity, parallel to the bottom wall. That inlet velocity is 10 m/s and it is associated to a Reynold's number of 50, hence no significant turbulent effects should be observed. The properties of both plate and fluid domains are

presented in Table 3. The dimensions concerning the domain of the simulation can be consulted in Figure 9, with the respective coordinate system and boundary conditions.

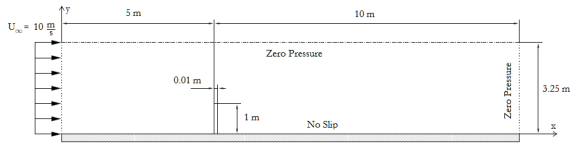

Figure 9: Benchmark simulation setup for clamped vertical plate [9].

Table 3: Properties of the plate and of the fluid domain [9].

	Fluid	**Plate**
Density, ρ $[kg/m^3]$	1	1200
Poisson ratio, υ	-	0.32
Young modulus, E $[GPa]$	-	3.5
Dynamic viscosity, μ $[Pa \cdot s]$	0.2	-
Moment of inertia, I $[m^4]$	-	8.3E-10

5.1. Structural Models

Regarding the structural portion of this study, three different models are constructed:

1. **Solid Model (SM)**: a reference case with SOLID186 elements from the Finite Elements package ANSYS© Mechanical APDL with 421 nodes.
2. **Beam ANSYS© Model (BAM)**: a flexible plate with BEAM4 elements, with structural data originated from ANSYS© as well.
3. **Beam Solver Model (BSM)**: a flexible representation of the plate with beam elements generated by the beam solver, using a *.beam* file as input.

In regards to the conceptualization of the beam model, its grid is centered in the geometric center of the plate, which coincides with the elastic axis in this case. The mesh from the SM case is adopted as the outer grid in both BAM and BSM cases.

5.2. Tip displacement and response frequency

Initially, the simulations are computed with 200 beam elements, with each element presenting a size of $0.005m$ along the y axis, and 421 outer structural nodes. The body's movement is simulated during 10 seconds, at the end of which the plate has a well defined stabilized deflection. This is achieved thanks to the viscous damping of the motion, resultant of the interaction of the plate with the surrounding air flow.

Evaluating the tip displacements during that period of time, with a time step of 0.01 seconds, the Figure 10 is obtained. Through its plot, the developed module data is shown to be an adequate replacement for the one generated by ANSYS©, as both cases present an identical behavior to each other. Slight deviations from the SM are observed, with the beam models reaching an equilibrium displacement of 0.0223 m, instead of x= 0.0243 m, like in the SM case and other studies of the benchmark. In this initial study, these differences may be attributed to lack of discretization of the structural grids, since the employed algorithm that transfers displacements and loads between those same meshes lacks robustness.

This fact may also be in the root of the low efficiency of the beam simulations when compared with the solid elements, as the outer mesh can create quite irregular shapes after its displacements update, hindering the convergence of the code. Counting the number of outer iterations of each test case, the SM concluded its simulation with 153254 iterations, while the BAM and BSM took 309054 and 309440 iterations, respectively.

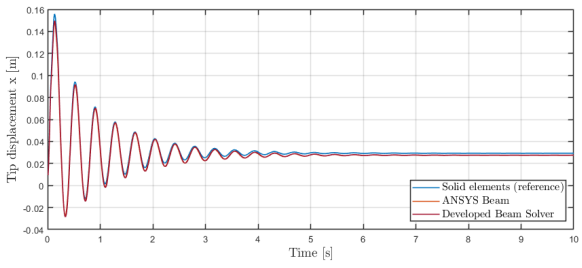

Figure 10: Tip displacement obtained from different models of the plate.

The evolution of the plate is depicted in figure 11, representing the deformation of the BSM model at distinct time steps. Firstly, at t=0.03 s, it is possible to identify a large pressure in the frontal area, where the inlet flow first collides with the body at study, and a lower pressure region close to the other side of the plate, where a separated region of the flow appears, due to the forcing of the fluid into the corner of the body, where a singularity of the NS equations occurs. This region increases its dimension, while the center of the generated vortex moves away from the plate, at t=0.13 s. Eventually, the properties of the structure and the flow become independent from time, around t=6.00 s, which yields approximately steady results.

Considering that the plate vibrates most significantly within the first 5 seconds of the simulation, a Fast Fourier Transform (FFT) with a Hanning window is applied to the computed BSM tip displacements, for a time step of 0.01 seconds. The

plot in Figure 12 is obtained, where the response frequency extracted from the marked peak corresponds to 2.73438 Hz. The SM and BAM responses have resulted in this same frequency as well, with very similar logarithmic decrements and damping ratios.

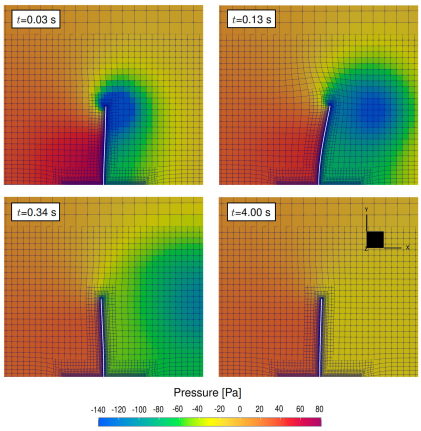

Figure 11: Plate response at relevant time steps, for the BSM simulation.

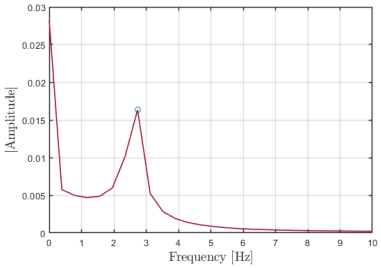

Figure 12: Single sided amplitude spectrum with a time step of 0.01 seconds.

Additionally, the developed beam solver was simulated with and without considering the implemented rotation degrees of freedom but the results yielded negligible differences, from which one can infer that this feature is not impactful in the interface update of the benchmark.

5.3. Discretization of structural grids

A study on the effect of the refinement of the structural meshes is then conducted, in order to assess its effects on the accuracy and performance of the beam simulations. For this effect, the grids presented in Tables 4 and 5 are created.

The meshes O1, O2, O3 and O4 have 257, 421, 1465 and 1620 nodes, respectively. Combining these different levels of refinement from both structural grids, the results are the most accurate, as one would expect, for high refinement from both (conjunction O4-B4, with a deviation of 1% from the SM case, in regards to the equilibrium position). It is inferred from this study that the refinement of the beam grid doesn't have a strong influence on the accuracy of the results, while the outer mesh has a predominant impact on that aspect, presenting limitations nonetheless when working with much coarser beam grids in the spanwise direction. This sets a precedent on how to handle the blade of the DTU 10 MW RWT, in which the beam should present a dense refinement in comparison with the outer mesh in that direction, with the intent of avoiding divergence situations where negative volume cells are reached, due to the irregularity of the updated outer mesh.

The refinement of any of the structural grids should not have much consequences in the performance of the simulations, as the number of outer iterations doesn't vary much with the distinct tested combinations of grids.

Table 4: Generated beam grids, with different discretization.

Beam grid	**Number of el.**	**El. y size [m]**
B1	50	0.020
B2	100	0.010
B3	200	0.005
B4	500	0.002

Table 5: Different outer structural grids used in this portion of the study, with respective dimensions of each element.

Outer grid	**Size x[m]**	**Size y[m]**	**Size z[m]**
O1	0.005	0.02	0.005
O2	0.0025	0.02	0.0025
O3	0.0025	0.01	0.0025
O4	0.0025	0.005	0.0025

6. DTU 10MW Turbine

The study of the full-scale rotor of the DTU 10MW RWT is centered around two distinct simulations: one where the geometry is considered rigid and another where one of the blades is flexible, using the FSI module of ReFRESCO in tandem with the developed beam solver.

The selected inlet velocity for all simulations corresponds to the rated wind speed of the turbine, 11.4 m/s. In what concerns the rotation velocity of the rotor, the value of -0.959 rad/s, relative to the x axis (refer to Figure 13), is selected and provides reference results from Castro [10], since the same speed is used in his work. The adopted time step for the simulations is 0.145596 seconds, which, considering the angular speed of the rotor, should lead to a rotation of approximately 8° per time step.

6.1. Fluid model

Multiple fluid grids, recurring to an AFM approach and to SG, are constructed, in order to evaluate their applicability to the FSI simulation. The chosen domain dimensions are presented in Figure 13, where the dotted line represents the interface between SG. The AFM configuration has a similar domain but without that interface.

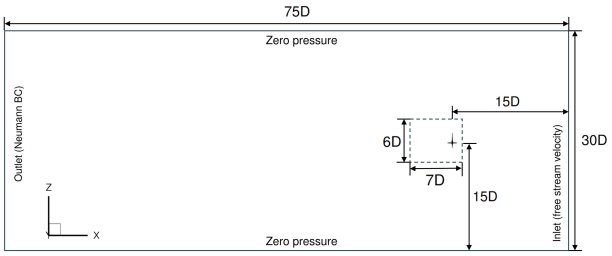

Figure 13: DTU 10MW RWT domain setup for the fluid grids (rotor not at scale).

In regards to the meshes themselves, the SG, already combining the two sub-domains, is constructed initially with approximately 13 million cells. For the generation of this mesh, a target y^+ is defined when introducing the viscous layer to the model, providing an adequate chance of solving of the boundary layer. Nevertheless, aiming at reducing the computational costs, wall functions are used to approximate the BL, instead of relying on the grid refinement near the wall. This approach considerably decreases the total number of cells to approximately 3.1 million. Finally, with the AFM approach, a specific refinement to the BL is also not carried out, which leads to a mesh of approximately 3.1 million cells as well. These three grids are then introduced in rigid simulations, from which the resultant parameters are computed and presented in Table 6.

Table 6: Key parameters computed in the rigid simulations, regarding thrust $\boldsymbol{T}$, power $\boldsymbol{P}$ and respective coefficients.

Fluid mesh	$\boldsymbol{T}$[MN]	$\boldsymbol{C_T}$	$\boldsymbol{P}$[MW]	$\boldsymbol{C_P}$
SG with refinement of the BL	1.94	0.977	9.78	0.432
SG with less refinement of the BL	1.90	0.955	10.10	0.446
AFM with less refinement of the BL	1.97	0.991	11.31	0.499

Comparing these values with Castro's [10], it is founded that both methods appear to provide reasonable results for the intended purposes of this work: testing the new FSI implementation quickly, with large simplifications, specially the modeling of the BL with wall functions. Nevertheless, SG are the most versatile ones, since they can be used in real life configurations with bodies that are moving and others that are static. In the case of AFM, one is limited to use them with geometries that move all at the same speed, which precludes the inclusion of tower-rotor interactions in future works, for example.

6.2. Flexible model

In what concerns the structural model of the blade, it is created based on properties of defined cross sections, presented in an input file of HAWC2 regarding the reference blade geometry. These discrete parameters are then made continuous by curve-fitting functions, which allows a denser refinement of the model. In what concerns the outer mesh, the points constituting various cross sections, extracted from the geometry supplied by MARIN, are adopted.

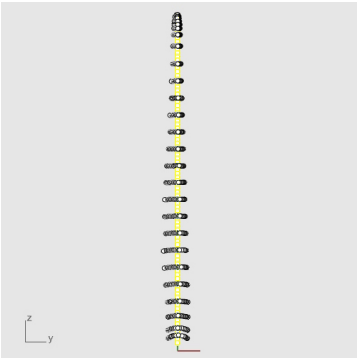

Figure 14: Beam grid (in yellow) and outer mesh (white dots) of the structural model of the blade.

A modal analysis of the body was then conducted. It presented some deviations from reference results in some of its modes, which could be explained by a deficient calculation of the shear center coordinates of the cross sections associated to each node, since that data was provided in function of the location of the center line, that is, a straight line that unites points at the half chord of each considered cross-section. The lack of discretization of these center lines, in comparison with the 50 available cross sections of the blade, may have led to errors in the computation of the variables that are dependent on it. Nevertheless, this model should still be able to portray fairly well the behavior of the DTU 10 MW RWT blade in an FSI simulation.

It must be recognized that the results of the simulation of the DTU 10MW RWT flexible rotor were not obtained by the date of the conclusion of this work, due to the non-parallelisation of the code, imposed by the new interface coupling. Only running on one processor, this condition hindered drastically the calculations of the simulation.

7. Conclusions

The present work expands the functionalities of ReFRESCO's FSI module in two major fronts. Firstly,

an interface between beam models and CFD grids is implemented. Aiming at avoiding extensive modifications of the main code, the RBF interpolation is used in the interface between the fluid domain and a new outer structural mesh that coincides with the outer surface of body. This latter grid is thus an intermediary of displacements and loads between the fluid and an inner beam grid, positioned on the elastic axis of the body. The update of the interface is also expanded to degrees of freedom of rotation, in which the node's coordinate system is rotated at each outer iteration based on the angle computed in the previous one.

Secondly, a Computational Structural Dynamics Model with beam elements is created, aiming to establish a user friendly way of setting up the structural model in the FSI simulations, without the need to recur to external software, namely ANSYS©. This solver is developed in an adjunct module of the main code and it is successfully verified and validated through static and modal analysis.

Afterwards, both developments are validated with a benchmark in an FSI context. The beam solver presents itself as an accurate replacement for ANSYS© in the generation of structural data, with its results showing a good agreement not only with the BAM case, but also with the SM one. The implementation of the rotational degrees of freedom in the interface update is deemed negligible in the benchmark study but its importance should be reassessed in future works. A study on the effect of the structural grid discretization on the accuracy and performance of the beam simulations is then conducted, combining different levels of refinement from both beam and outer grids. The outer mesh discretization had a predominant impact on the accuracy of the simulations, presenting limitations nonetheless when working with much coarser beam grids in the spanwise direction. The various discretizations don't have a significant effect on the performance of the simulations, without large variations of the total number of outer iterations.

Finally, a set up for the simulation of the DTU 10MW rotor is developed, with the execution of a rigid simulation using the AFM and SG approach for its domains. A structural beam representing a blade of the DTU 10MW is also created with the developed beam module, based on the interpolation of known values concerning its material and geometrical properties. Results for a DTU 10MW RWT flexible rotor simulation were not obtained by the date of the conclusion of this work, due to the non-parallelisation of the code, imposed by the new interface coupling.

Future works should focus on establishing a more robust coupling between the beam and outer structural grids, while also performing the parallelisation of the code, in order to make the simulations' computational costs reasonable.

Acknowledgements
The author would like to thank WavEC, blueOASIS and its engineers, for providing the necessary means and proper formation that allowed the completion of this work.

References

[1] Dong Ok Yu and Oh Joon Kwon. Predicting wind turbine blade loads and aeroelastic response using a coupled CFD-CSD method. *Renewable Energy*, 70:184–196, 2014.

[2] Laurette Bronswijk. *Fluid-Structure Interaction Of Self-Adaptive Marine Propellers Using RANS-FEM Towards The Validation Of BEM-FEM.* Master's thesis in Marine Technology, TU Delft, 2017.

[3] MARIN. *ReFRESCO Theory Manual v2.4.0*, October 2017. Version 1.0.

[4] SH Jongsma, E.T.A van der Weide, and Jaap Windt. Implementation and verification of a partitioned strong coupling Fluid-Structure Interaction approach in a finite volume method. *Tecnical Report MARIN Academy*, 2016.

[5] A.de Boer, A.H.van Zuijlen, and H.Bij. Comparison of conservative and consistent approaches for the coupling of non-matching meshes. *Department of Aerospace Engineering, Delft University of Technology*, 197(49):4285–4297, 2008.

[6] J. N. Reddy. *An introduction to the Finite Element Method.* Mc Graw Hill, 2006.

[7] ANSYS Inc. *Theory reference for the Mechanical APDL And Mechanical applications*, Release 12.0, 2009.

[8] Guilhaume de Nayer. *Interaction Fluide-Structure Pour Les Corps Élancés.* PhD thesis, École Centrale de Nantes (ECN), 2008.

[9] Herry Lesmana. *Contribution To Numerical Modeling Of Fluid-structure Interaction In Hydrodynamics Applications.* Master's thesis in Computational Mechanics, École Centrale de Nantes, 2011.

[10] Ivan David Rojas Castro. *Design Of A 10MW Wind Turbine Rotor Blade For Testing Of A Scaled-down Floating Offshore Support Structure.* Master's thesis in Sustainable Energy Technology, TU Delft, 2017.